S-Nitrosylation of Platelet $\alpha_{IIb}\beta_3$ As Revealed by Raman Spectroscopy†

Geraldine M. Walsh,‡ Deirdre Leane,§ Niamh Moran,‡ Tia E. Keyes,§ Robert J. Forster,§ Dermot Kenny,‡,§ and Sarah O'Neill*,‡,§

Molecular and Cellular Therapeutics, Royal College of Surgeons in Ireland, Dublin 2, Ireland, and Biomedical Diagnostics Institute, Dublin City University, Dublin 9, Ireland

Received October 5, 2006; Revised Manuscript Received March 15, 2007

ABSTRACT: The exact mechanisms regulating conformational changes in the platelet-specific integrin $\alpha_{IIb}\beta_3$ are not fully understood. However, a role exists for thiol/disulfide exchange in integrin conformational changes leading to altered disulfide bonding patterns, via its endogenous thiol isomerase activity. Nitric oxide (NO) accelerates this intrinsic enzymatic activity and, in doing so, reverses the activational state of the integrin on the platelet surface toward a more unactivated one. We propose that it is an S-nitrosylation-induced "shuffling" of thiol/disulfide exchange that regulates this reversal of the activated state of the integrin. In this study, we use Raman spectroscopy to explore S-nitrosylation of purified $\alpha_{IIb}\beta_3$. Using *S*-nitrosoglutathione (GSNO) as a model system, we identify Raman markers which show a direct interaction between NO and the thiol groups of the integrin and reveal many of the structural changes that occur in $\alpha_{IIb}\beta_3$ in the course of not only its activation but also its deactivation. Key conformational changes are detected within the integrin when treated with manganese (Mn^{2+}), occurring mainly in the cysteine and disulfide regions of the protein, confirming the importance of thiol/disulfide exchange in integrin activation. These changes are subsequently shown to be reversed in the presence of NO.

Aggregation of platelets is a crucial process in the hemostatic and thrombotic systems. A critical step in platelet aggregation is the activation of the platelet-specific integrin $\alpha_{IIb}\beta_3$ (*1*). In its native, resting state, $\alpha_{IIb}\beta_3$ has a low affinity for its primary ligand fibrinogen. Upon platelet activation, it undergoes dramatic conformational changes, which increases its affinity for its primary ligand fibrinogen. Fibrinogen binding facilitates cross-linking of adjacent platelets to form a thrombus. Despite the pivotal role of $\alpha_{IIb}\beta_3$ in thrombotic disorders, the exact molecular mechanisms of this conformational switch are not yet fully elucidated.

$\alpha_{IIb}\beta_3$ has an endogenous enzymatic thiol isomerase activity (*2*), which catalyzes thiol/disulfide bond exchange within the molecule and is hypothesized to be involved in conformational changes. Recent evidence suggests that $\alpha_{IIb}\beta_3$ and its thiol isomerase activity are targets for redox regulation (*3*−*5*). Divalent Mn^{2+} cations induce an active-like conformation in $\alpha_{IIb}\beta_3$, which increase ligand binding (*6*−*8*). Nitric oxide (NO),[1] alone or in combination with glutathione (GSH), reversed this activation state by directly targeting $\alpha_{IIb}\beta_3$ in platelets. NO also accelerated the thiol isomerase activity of purified $\alpha_{IIb}\beta_3$ in an allosteric manner (*4*). We therefore hypothesized that the effect of NO on $\alpha_{IIb}\beta_3$ may occur as a direct interaction between it and the integrin. It is increasingly emerging that modification of proteins by NO, a process known as S-nitrosylation, is a functionally relevant posttranslational modification that plays a key role in a wide variety of cellular functions.

Techniques such as protein crystallography have greatly enhanced the understanding of integrin structure (*9*−*11*). However, this technique is constrained by its static nature and the uncertain relevance of the crystallized structure to the form the protein takes in fluid media. For that reason, we sought an alternative approach to explore the structural changes accompanying the activation of $\alpha_{IIb}\beta_3$ in a biologically relevant setting. We used Raman spectroscopy, a noninvasive tool, which has proven useful in determining the conformation and molecular structure of proteins in aqueous media. There are a limited number of descriptions of Raman spectroscopy as applied to glycoproteins and integrins (*12*−*16*). Furthermore, resonance Raman has been widely used to explore ligand binding and heme distortion in heme proteins, including myoglobin, nitric oxide synthase, and soluble guanylate cyclase (*17*−*20*).

Raman spectroscopy is one of the few techniques that can unambiguously detect the presence of disulfide bonds in proteins (*21*). Indeed, this technique is remarkably sensitive to the geometry about disulfide bonds in proteins and peptides. Since disulfide rearrangement is of significant importance in the regulation of $\alpha_{IIb}\beta_3$ activation states (*22*), we considered Raman spectroscopy an ideal tool to explore changes in the thiols and disulfides in the integrin. In this study we show that Mn^{2+} dramatically alters specific areas of the secondary structure of purified $\alpha_{IIb}\beta_3$. We describe how NO converts Mn^{2+}-activated $\alpha_{IIb}\beta_3$ to a conformation

† This work was supported by the Science Foundation Ireland, Grants 04/BR/B0666 and 05/INI/B30, the Health Research Board Ireland, and the Higher Education Authority.

* Corresponding author. Telephone: +353-1-402 2349. Fax: +353-1-402 2453. E-mail: soneill@rcsi.ie.

‡ Royal College of Surgeons in Ireland.

§ Dublin City University.

[1] Abbreviations: EDTA, ethylenediaminetetraacetic acid; GSH, glutathione; GSNO, *S*-nitrosoglutathione; Mn^{2+}, manganese; NO, nitric oxide; PVDF, polyvinyl difluoride; SDS−PAGE, sodium dodecyl sulfate−polyacrylamide gel electrophoresis; SNOAC, *S*-nitroso-*N*-acetylcysteine.

10.1021/bi0620712 CCC: $37.00
Published on Web 05/03/2007

similar to a resting conformation of the integrin. The Raman studies further indicate that NO directly modifies $\alpha_{IIb}\beta_3$ at its thiol groups, a finding consistent with our hypothesis that $\alpha_{IIb}\beta_3$ can be directly S-nitrosylated. Direct S-nitrosylation of $\alpha_{IIb}\beta_3$ has not previously been demonstrated, and this finding provides a mechanism for the previously observed effects of NO on integrin activation. The result of this Raman study was confirmed using the biotin-switch assay (*23*) to verify in vitro nitrosylation of integrin cysteines and was further supported by the presence of known nitrosylation motifs in the primary amino acid sequence of $\alpha_{IIb}\beta_3$.

EXPERIMENTAL PROCEDURES

Materials. Monoclonal antibodies, fluorescein isothiocyanate- (FITC-) conjugated monoclonal antibody PAC-1, and phycoerythrin- (PE-) conjugated monoclonal antibody CD62P were obtained from Becton Dickinson, Oxford, England. Glutathione reduced (GSH), *S*-nitrosoglutathione (GSNO), and Ultrafree-MC microcentrifuge filters (10000 NMWL) were purchased from Sigma Aldrich Ltd., Tallaght, Ireland. $\alpha_{IIb}\beta_3$ was obtained from Enzyme Research Laboratories, Swansea, U.K. The Bradford DC assay and micro-Bio-Spin P6 columns were obtained from Bio-Rad Laboratories Ltd., Hertfordshire, U.K. The CM5 dextran-gold (Au) sensor chip was from Biacore, Uppsala, Sweden. The SuperSignal West Pico Chemiluminescent kit was from Pierce, Rockford, IL.

FACS Analysis of PAC-1 and P-Selectin Expression. Gel-filtered platelets, prepared as described previously (*4*), were adjusted to 3×10^8 platelets/mL and diluted 1:1 in buffer. Platelets were activated with 1 unit/mL thrombin for 3 min at 37 °C. The activated platelets were immediately incubated with GSH (3 mM) ± *S*-nitroso-*N*-acetylcysteine (SNOAC, 10 μM) for 3 min at room temperature. The platelets were incubated with both fluorescein isothiocyanate- (FITC-) conjugated monoclonal antibody, PAC-1, which is directed against an active conformation of $\alpha_{IIb}\beta_3$, and phycoerythrin- (PE-) conjugated monoclonal antibody, CD62P, directed against P-selectin, which is only expressed on the platelet surface upon activation and secretion. Samples were fixed with 1% formaldehyde and read at room temperature on a Becton-Dickinson FACScan flow cytometer at 488/510 nm. Platelet populations were gated, and mean fluorescent histograms were generated for each sample.

Flow Cytometry Data Analysis. Unactivated platelets were marked at a value of 5% positive for both PAC-1 and CD62P expression. All subsequent samples were measured relative to the 5% gate in the resting samples, giving a percentage positive score for each antibody and for each treatment. Log-transformation was used to resolve nonnormality of the data (Shapiro-Wilks *P*-value = 0.1794 and 0.3271 for PAC-1 and CD629P, respectively), and *p*-values were adjusted using the Bonferroni correction.

Preparation of $\alpha_{IIb}\beta_3$ for Raman Spectroscopy. $\alpha_{IIb}\beta_3$ was concentrated by centrifugation at 4000*g* for 30 min at 4 °C through Ultrafree-MC microcentrifuge filters (10000 NMWL) prewashed with buffer. The protein was exchanged into a PBS buffer (40 mM Na_2HPO_4, 10 mM $NaH_2PO_4{\cdot}H_2O$, 100 mM NaCl, pH 7.4) containing 0.1% Triton X-100 (PBSTX), which gives a minimal level of background signal in Raman spectroscopy. The protein solution was carefully washed off the filter membrane, and protein concentration was determined using the Bradford DC assay. Concentrations of greater than 10 mg/mL were found to be suitable for Raman spectroscopy.

Analysis of Purified $\alpha_{IIb}\beta_3$ by Raman Spectroscopy. A 1 μL drop of concentrated $\alpha_{IIb}\beta_3$ was placed on a CM5 dextran-gold (Au) chip; surface roughness was estimated to be approximately 2. The Raman spectra were recorded on a HORIBA Jobin Yvon LabRAM HR 2000 spectrometer, equipped with an integral confocal microscope. A 632.8 nm excitation line was employed from an air-cooled HeNe laser. The scattered radiation was observed with 180° geometry with a cooled (−75 °C) charged-coupled device (CCD) detector. The laser beam was focused through a 300 μm confocal hole onto a spot of 1 μm in diameter with a long focal length objective of the order of 10×. Data acquisition times were every 6 s with 20 accumulations. The holographic grating (1800 grooves/nm) allowed resolution of 0.1 cm^{-1}. The instrument was calibrated using silicon wafer (520 cm^{-1}) and acetonitrile standards. Accuracy was estimated to be less than 0.5 cm^{-1}. Laser power was limited, using optical density to 23 mW to minimize the possibility of damage to the protein. Spectra of blank PBS buffer with 0.1% Triton X-100 were collected and used for background subtraction. Solid GSH and GSNO were analyzed in their solid state on a low-fluorescence glass slide for acquisition of Raman spectra. Spectra were analyzed using Peak Fit or Labspec software.

Treatment of $\alpha_{IIb}\beta_3$ with Conformation Modifying Reagents. Purified, concentrated (>10 mg/mL) $\alpha_{IIb}\beta_3$ was treated with 10 mM NO donor, *S*-nitrosoglutathione (GSNO), in the dark at room temperature for 15 min. The samples were centrifuged through micro-Bio-Spin P6 columns equilibrated with PBSTX buffer to remove any excess GSNO from the sample. A 1 μL drop of the modified protein was placed on the dextran-modified Au chip, and Raman spectra were acquired as described above. Similarly, purified and concentrated $\alpha_{IIb}\beta_3$ in PBSTX buffer was treated with 1 mM $MnCl_2$ for 10 min at room temperature. One microliter of this modified protein was placed on the Biacore dextran-Au chip and analyzed as described. The remainder of the sample was treated with 10 mM GSNO for 15 min at room temperature in the dark. The sample was spun through micro-Bio-Spin P6 columns equilibrated with PBSTX buffer to remove any excess GSNO. A 1 μL drop of this Mn^{2+}-activated, GSNO-treated $\alpha_{IIb}\beta_3$ was placed on the Biacore dextran-Au chip for Raman spectra acquisition. All measurements were carried out a minimum of $n = 3$ and showed excellent reproducibility.

Biotin-Switch Assay of Purified $\alpha_{IIb}\beta_3$. Purified $\alpha_{IIb}\beta_3$ (3 mg/mL), in a final volume of 50 μL, was incubated with deionized H_2O or the NO donor SNOAC (1 mM) for 20 min at room temperature. Nitrosylation was then detected using a modified version of the biotin-switch assay (*23*, *24*). Briefly, samples were incubated with 150 μL of blocking solution [9 volumes of HEN buffer (25 mM HEPES, pH 7.4, 0.1 mM EDTA, 10 μM neocuprione), 1 volume of 25% SDS/20 mM MMTS (added from a 2 M stock prepared in DMF)] at 50 °C for 1 h. Four hundred microliters of cooled (−20 °C) acetone was added to the samples, and they were precipitated twice. After the final precipitation, the pellets were carefully resuspended in 30 μL of HENS solubilization buffer (25 mM HEPES, pH 7.4, 0.1 mM EDTA, 10 μM

neocuproine, 1% SDS), and 2.4 μM ascorbate and 1 mM biotin−HPDP were added to each sample, and they were vortexed vigorously. Samples were incubated at room temperature in the dark for 1 h. To detect biotinylated proteins by western blot, an equal volume of 2× nonreducing sample buffer was added to each sample; they were not boiled and were run on 7.5% SDS−PAGE. Proteins were transferred to PVDF membrane, stained with the reversible protein stain Ponceau-S, and imaged. The membrane was then blocked for 1.5 h in 1% casein in 0.05% PBS Tween-20 (PBST) and probed with 1:4000 anti-biotin antibody and 1:20000 dilutions of goat anti-mouse HRP. Membranes were developed using the SuperSignal West Pico Chemiluminescent kit and exposed to Kodak Biomax ML film.

RESULTS

NO and GSH Reverse PAC-1 Binding to Thrombin-Activated Platelets. Addition of thrombin (1 unit/mL) to platelets causes an increase in the binding of both PAC-1 and CD62P, indicating activation of the integrin $\alpha_{IIb}\beta_3$ and the platelet, respectively (Figure 1). Following activation, treatment alone with the *S*-nitrosothiol *S*-nitroso-*N*-acetyl-cysteine (SNOAC, 10 μM) had no significant effect on either PAC-1 or CD62P binding, respectively (Figure 1A,B). In contrast, addition of GSH to the thrombin-activated platelets causes a significant reversal in PAC-1 binding (Figure 1C) while having no effect on CD62P binding (Figure 1D). Interestingly, addition of a combination of the two compounds caused a large, highly significant reduction in PAC-1 binding (Figure 1E). Despite these effects on the integrin, the platelet remains activated throughout, as the level of the binding of CD62P remained elevated (Figure 1F). The bar chart in Figure 1G ($n = 3$) shows a 78% reduction in PAC-1 binding ($p < 0.001$) in activated platelets treated with a combination of SNOAC and GSH, greater than the effect seen with either SNOAC alone (8%) or GSH alone (54%), indicating an additive effect of the two compounds. Activated platelets treated with GSH alone had a reduction in the binding of Pac-1 by approximately 54% ($p < 0.05$) when compared to the thrombin-activated platelets. No effect on CD62P binding to the activated platelets was observed.

Distinguishing between Nitrosylated and Free Thiols by Raman Spectroscopy. The Raman spectroscopic analysis of solid glutathione (GSH) and solid *S*-nitrosoglutathione (GSNO), its S-nitrosylated derivative, was studied as simple analogues of S-nitrosylated cysteines, in order to identify marker bands of S-nitrosylation in proteins. The Raman spectra are shown in Figure 2. Assignments are made on the basis of comparison with related functionalities and on the basis of computed normal coordinate analysis using Gaussian 98 (*25*). A broad, weak feature at 1526 cm^{-1} and a feature of modest intensity at 1385 cm^{-1} are assigned to the N═O stretch, and a split band at approximately 1103 cm^{-1} is assigned to the SN stretch. A feature at 886 cm^{-1} is attributed to the SNO bend mode. The most intense new feature in the NO-bound derivative is the sharp and intense peak at 520 cm^{-1}, which is attributed to an SN stretch mode. Additional features at 312 and 260 cm^{-1} are assigned to torsion and SNO bend modes, respectively. Other prominent features at 436 and 462 cm^{-1} appear or are significantly enhanced in intensity compared with GSH. In the C−S region, 620 and 680 cm^{-1} are also strongly impacted by NO

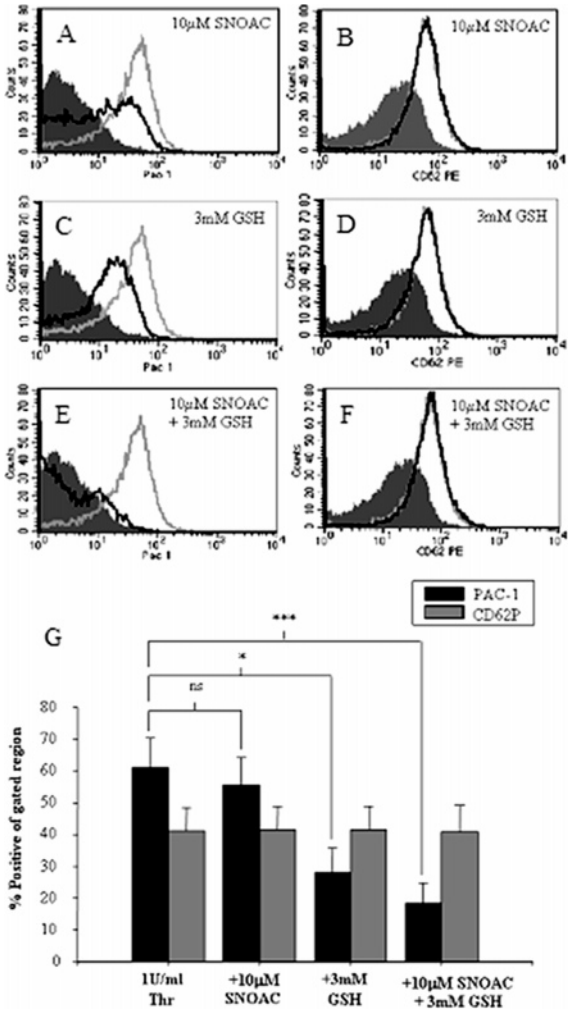

FIGURE 1: NO and GSH reverse integrin activation in thrombin-activated platelets. Gel-filtered platelets, activated with 1 unit/mL thrombin, were treated with SNOAC (10 μM) and GSH (3 mM), alone or in combination, and labeled with PAC-1 and CD62P antibodies. The unactivated population is indicated in solid gray, thrombin activation is shown by the light gray line, and the effect of the treatment is shown by the black line. (A) Representative histograms showing the effects of SNOAC alone on PAC-1 and (B) CD62P binding, respectively, after activation with thrombin. (C) Effects of GSH alone on PAC-1 and (D) CD62P binding, respectively, after activation with thrombin. (E) Effects of a combination of SNOAC and GSH on Pac-1 binding and (F) CD62P binding to the activated integrin. (G) A graph of the mean of $n = 3 \pm$ SEM.

binding (Figure 2A,B). For GSH a very prominent band at approximately 2526 cm^{-1} is assigned to the SH stretching mode of the cysteine sulfhydryl (Figure 2C). In contrast, for solid GSNO this band is not present (Figure 2D). This is expected, as in GSNO the free thiol of the cysteine in GSH has been deprotonated and replaced with an NO group upon nitrosylation. Overall, there is significant spectral perturbation of the vibrational spectrum of GSNO spectra compared to GSH. This indicates that Raman spectroscopy is indeed a useful method to study the posttranslational modification of proteins by NO.

Treatment of Mn^{2+}-Activated $\alpha_{IIb}\beta_3$ with GSNO Results in a Native-like Conformation of the Integrin. The Raman spectra of unactivated, native $\alpha_{IIb}\beta_3$, Mn^{2+}-activated $\alpha_{IIb}\beta_3$, and Mn^{2+}-activated $\alpha_{IIb}\beta_3$ in the presence of NO are shown in Figure 3. In the native protein, in the lower wavenumber

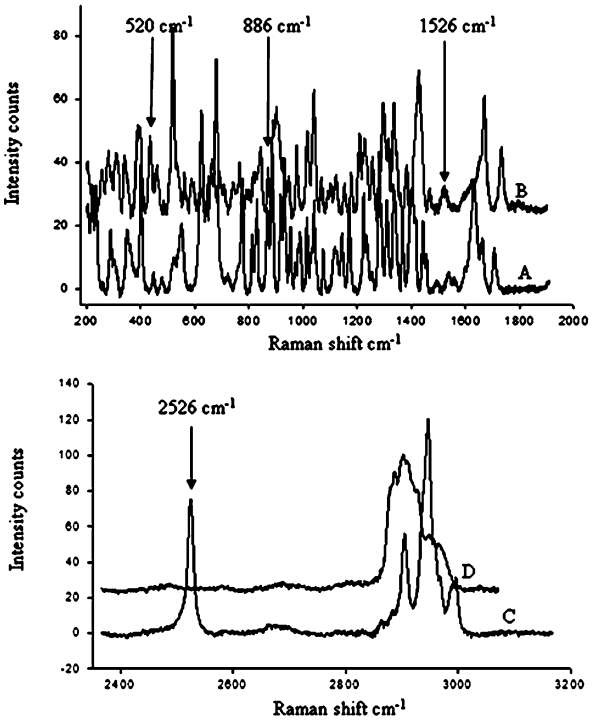

FIGURE 2: Raman spectra of GSH and GSNO in the solid state. (A) The lower wavenumber region of solid GSH. (B) The lower wavenumber region of solid GSNO. The most notable features are indicated by arrows. (C) A very prominent band at approximately 2526 cm^{-1} in GSH is assigned to the SH stretching mode of the cysteine sulfhydryl. (D) In contrast, for solid GSNO this band is not present.

region (Figure 3A), the S−S stretching region was deconvoluted. The frequencies of these vibrations are highly sensitive to the extent of internal rotation about the C−S bond in the cysteine C-C-S-S-C-C network. The 474, 486, and 494 cm^{-1} modes are assigned to conformationally strained rotamers of the C-C-S-S-C-C motif with a dihedral angle ranging from approximately 16° to 29° (*26*). The 505 cm^{-1} feature is assigned to the *gauche*−*gauche*−*gauche* cysteine rotamer. The remaining disulfide features at 518, 524, and 530 cm^{-1} are assigned as *gauche*−*gauche*−*trans* and *trans*−*gauche*−*trans* rotamers in which the dihedral angle is approximately 85°. The complexity of this spectral region is consistent with the cysteine-rich nature of the protein and confirms that the majority of sulfhydryls participate in disulfide bonds. It also suggests considerable heterogeneity across these bonds and that a significant number are sterically strained in the native protein. Such conformation about the S−S are relatively unusual but have been reported previously, for example, in the α_1-acid glycoprotein (*15*). In the absence of the SERS substrate, at >10 mg/mL of $\alpha_{IIb}\beta_3$, the Raman signature for the protein was prohibitively weak, with poor signal to noise ratio. The use of a dextran-coated gold substrate enhanced the Raman signal from the integrin by approximately 2 orders of magnitude compared with a free solution of the integrin, with a comparable increase in signal to noise ratio. The signal was reproducible across the substrate where integrin had been administered. It is noted that there is no apparent evidence for direct interaction of disulfides or thiols with the gold substrates. If so, we would expect this to be manifested by disproportionate intensities in vibrational modes associated with, for example, C−S vibrations. Even when bare metal

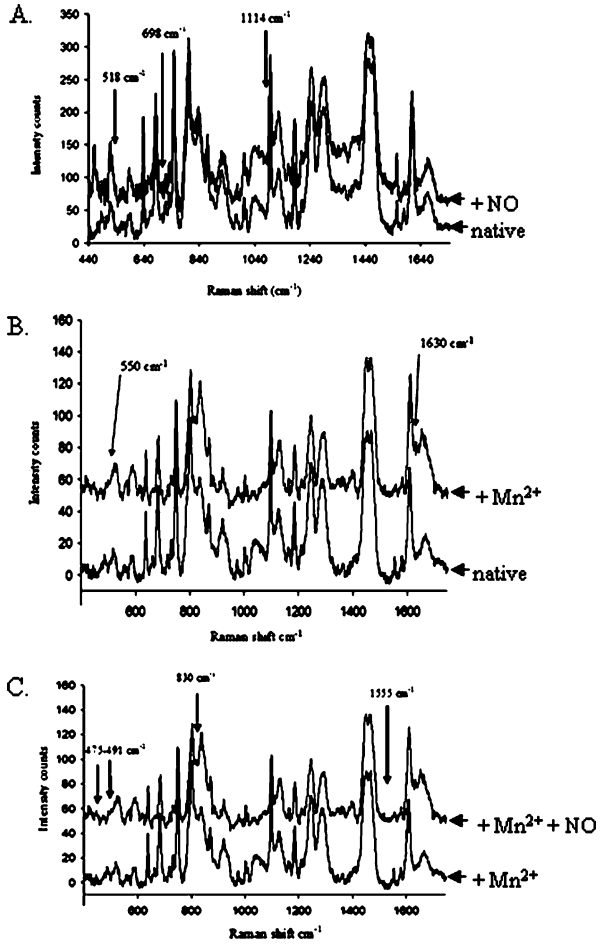

FIGURE 3: (A) Comparison of the Raman spectra of native $\alpha_{IIb}\beta_3$ and $\alpha_{IIb}\beta_3$ treated with GSNO. Shown is an overlay of the spectrum of native $\alpha_{IIb}\beta_3$ with the spectrum of NO-treated $\alpha_{IIb}\beta_3$. The features at 518 and 1114 cm^{-1} in the NO-treated integrin are attributed to S−N stretch modes. The feature at 698 cm^{-1} is a new mode not present in the native integrin. (B) Exposure of $\alpha_{IIb}\beta_3$ to Mn^{2+} causes conformational changes within the integrin. In the Mn^{2+}-treated $\alpha_{IIb}\beta_3$, there is a general shift in the S−S stretch envelope to higher energy. The lowest frequency feature at 474 cm^{-1} associated with the strained conformer is lost. New features appear at 500 cm^{-1} and around 537 and 545 cm^{-1}, indicating an overall reduction in strain on the cysteine bonds. (C) Mn^{2+}-activated $\alpha_{IIb}\beta_3$ reverts back toward the native integrin in the presence of NO. A reversion of the bonds to their native state occurs with the reappearance of the strained S−S bands at 475 and 491 cm^{-1}. The band at 830 cm^{-1} is attributed to a SNO bend. The band at 1555 cm^{-1} is attributed to the N═O stretch.

surfaces were employed with the integrin (*14*), significant enhancement in the aromatic modes not associated with the thiol was observed. This suggests that the cysteines are sufficiently buried in the protein structure to prevent interaction with the surface. In this instance, we believe that the dextran supports the protein within 50 nm of the metal without permitting nonspecific adsorption.

In the presence of NO there is enhancement of the intensity of a feature at 518 cm^{-1} which may be attributed to an S−N stretch mode and appearance of a weak mode at 830 cm^{-1} which may be due to SNO bending. A mode appears at 1114 cm^{-1} which may be attributed to the S−N stretch. Additional features around 420, 456, and 462 cm^{-1} appear in the NO-treated integrin spectrum but not in the native $\alpha_{IIb}\beta_3$. They correlate well with unassigned low-frequency modes observed for GSNO. New modes at 619 and 698 cm^{-1} are also

observed, and these modes do not appear in the purified integrin or in GSNO. The origin of these modes is unclear, but they may represent shifts in a small number of sulfhydryl C−S modes due to binding of NO. Concomitantly, in the S−H vibrational region, the weak SH modes appear to be lost on treatment of the integrin with GSNO. Therefore, while the exposure of integrin to NO appears to have little influence on the structure or conformation of the protein, there is evidence to suggest that NO binds to the few free SH groups available.

A number of subtle but key changes are observed in the Raman spectra of $\alpha_{IIb}\beta_3$ upon exposure to Mn^{2+} (Figure 3B). There is a general shift in the amide I feature centered between 1630 and 1700 cm^{-1} toward a lower frequency. The amide I band represents the sum of coupled amide and C═O stretch modes for the protein backbone and is very sensitive to protein conformation. The maxima of this broad envelope shifts from approximately 1670 cm^{-1} for the native integrin to approximately 1653 cm^{-1} for the Mn^{2+}-activated species, with concomitant enhancement of a feature at 1634 cm^{-1}, which is thought to be due to the presence of a β-sheet. This is indicative of conformational change within the protein structure and suggests broadly that the α-helical content has increased with associated alterations to the β-sheet content (*27*). Comparison with the amide III band (1230 and 1310 cm^{-1}), which comprises N−H and C−H deformation contributions, was not informative because of interference from the signal of the carbohydrate portion of the integrin.

Another key change following activation occurs in the S−S disulfide stretch spectral region between 450 and 550 cm^{-1}. The analysis of the Raman spectrum of native $\alpha_{IIb}\beta_3$ indicated that the majority of sulfhydryls form disulfide bonds and that some of these bonds are sterically strained in the native, unactivated integrin. However, following treatment with Mn^{2+} there is a general shift in the S−S stretch envelope to a higher energy. The lowest frequency feature at 474 cm^{-1} associated with the strained conformer is lost. New features appear at 500 cm^{-1} and around 537 and 545 cm^{-1}. This behavior, particularly the loss of the lowest frequency modes, indicates a reduction in strain at the cysteine sites on activation. There is little change, though, to the overall relative intensity of the S−S envelope. This indicates that few disulfides are converted to sulfhydryls, and rather a reshuffling of the S−S bonds appears to occur, with release of a small number of highly strained bonds.

Treatment of Mn^{2+}-activated $\alpha_{IIb}\beta_3$ with GSNO led to a number of changes compared to the Raman spectrum of the Mn^{2+}-activated $\alpha_{IIb}\beta_3$ (Figure 3C). Interestingly, these changes showed a reversal of the activated integrin structure, with a shift back to a more resting, native integrin structure. In particular, changes occurred about the disulfide spectral regions following NO treatment of Mn^{2+}-actviated $\alpha_{IIb}\beta_3$. There is some reversion of the bonds to the native state, with the reappearance of the strained S−S bands at 475 and 491 cm^{-1}. However, this does not appear to be complete as the 518 and 505 cm^{-1} features are not returned. In addition, relatively strong features between 450 and 500 cm^{-1}, similar to those observed for the native integrin treated with GSNO, appear. A band at 830 cm^{-1} attributed to the SNO bend for the GSNO-treated native $\alpha_{IIb}\beta_3$ also appears, and similar to the NO-treated native integrin, a band at 1555 cm^{-1} is

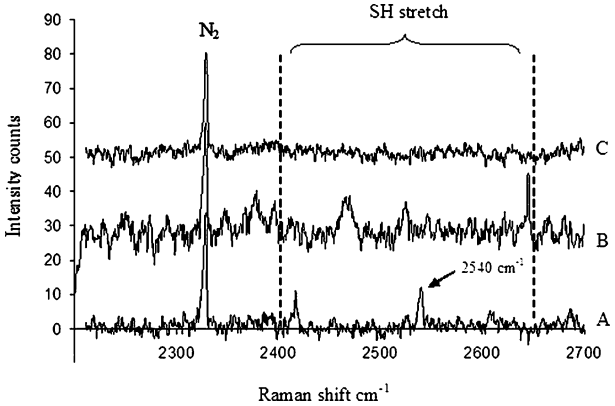

FIGURE 4: Comparisons in the SH region of $\alpha_{IIb}\beta_3$ reveal a loss of free thiols upon treatment with NO. Shown here is an expansion of the S−H spectral region focusing on the area between 2400 and 2650 cm^{-1}. (A) This is native $\alpha_{IIb}\beta_3$. A prominent SH mode is present at 2540 cm^{-1}. (B) This is the S−H region of $\alpha_{IIb}\beta_3$ treated with Mn^{2+}. The SH stretch at 2540 cm^{-1} appears to be lost with the appearance of broad weak bands at 2456, 2546, and 2625 cm^{-1}. (C) This is the SH region of Mn^{2+}-activated $\alpha_{IIb}\beta_3$ treated with NO. No band is present in the 2549 cm^{-1} region, thus indicating a loss of any free thiols in the integrin following treatment with NO.

apparent which is attributed to the N═O stretch. It should be pointed out that, although clear and reproducible, these features are necessarily relatively weak, because of the small number of residues in the overall, very large protein that are affected.

The SH Region of $\alpha_{IIb}\beta_3$ Reveals Direct Modification by NO. The SH stretch region for $\alpha_{IIb}\beta_3$ in its native state (A), following treatment with Mn^{2+} (B) and following treatment with Mn^{2+} and subsequent treatment with GSNO (C), is shown in Figure 4. The signal was normalized to the N_2 stretch mode for ambient nitrogen at 2330 cm^{-1}. Upon Mn^{2+} activation, the S−H stretch at 2540 cm^{-1} appears to be lost with the appearance of broad weak bands at 2456, 2546, and 2625 cm^{-1}. This suggests that both the number and nature of the free sulfhydryls have changed, but the small signal indicates that there is not a significant increase in the number of free sulfhydryls. This is consistent with the changes in the S−S binding region and suggests shuffling rather than extensive reduction of S−S bonds upon activation. Most tellingly, the SH stretch region is silent for the Mn^{2+}-activated integrin after GSNO treatment. This is in concurrence with the changes observed about the disulfides in NO-treated, Mn^{2+}-activated $\alpha_{IIb}\beta_3$ and is a key difference between the Mn^{2+}-activated and Mn^{2+}-activated, NO-treated $\alpha_{IIb}\beta_3$ as the broad SH band at approximately 2500 cm^{-1} is completely lost. This indicates a loss of any free thiols in the integrin following treatment with NO and is good evidence for direct interaction between NO and free thiol(s) of cysteines in $\alpha_{IIb}\beta_3$.

Analysis of the Amide Bands of $\alpha_{IIb}\beta_3$ Reveals Tertiary Conformational Changes upon Treatment with NO. The amide stretches of a protein are sensitive to environmental changes, and their structure depends on the population of the secondary structural elements. The amide I mode in a protein is primarily a C═O stretching band, which may have some contributions from CN stretching and CCN deformation. High-energy amide I ν(C═O) stretches are generally attributed to a β-sheet conformation, while lower energy (~1650 cm^{-1}) indicates α-helical structure. The amide I

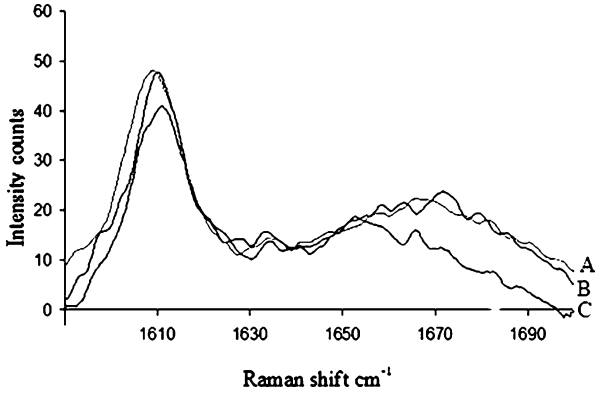

FIGURE 5: Tertiary conformational changes of $\alpha_{IIb}\beta_3$ occur upon treatment with NO. Shown here is an expansion of the amide I spectral region. (A) This is native $\alpha_{IIb}\beta_3$. (B) This is Mn^{2+}-$\alpha_{IIb}\beta_3$ where the changes are indicative of a change in the α-helical content of the protein. (C) This is Mn^{2+}-$\alpha_{IIb}\beta_3$ treated with NO. Here the amide I stretch is shifting to a higher frequency when compared to (B). This indicates that, upon nitrosylation, Mn^{2+}-activated $\alpha_{IIb}\beta_3$ reverts back toward a more native, resting conformation.

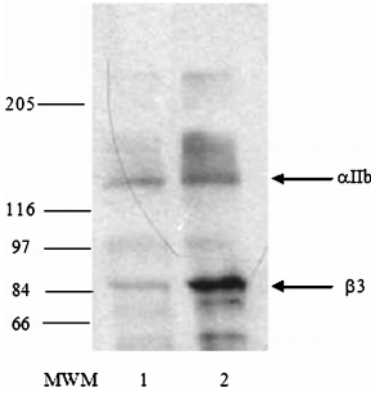

FIGURE 6: The biotin-switch assay shows nitrosylation of purified $\alpha_{IIb}\beta_3$. Concentrated, purified $\alpha_{IIb}\beta_3$ (3 mg/mL) in the absence (lane 1) or presence (lane 2) of 1 mM SNOAC was subjected to the biotin-switch assay. The increase in signal in the NO-treated lane indicates that nitrosylation of $\alpha_{IIb}\beta_3$ has occurred, with the most intense band at approximately 90 kDa, which corresponds to the approximate molecular mass of nonreduced β_3. This blot is a representative of four separate experiments. MWM are the molecular mass markers in kDa.

stretch of $\alpha_{IIb}\beta_3$ is shown in Figure 5. Activation of $\alpha_{IIb}\beta_3$ with Mn^{2+} causes a shift of the amide I stretch to a lower energy compared to native (B). Overall, the changes are indicative of an increase in the α-helical content of the protein on activation. In contrast, addition of NO to Mn^{2+}-activated $\alpha_{IIb}\beta_3$ shifts the amide I stretch to a higher frequency compared to Mn^{2+}-activated $\alpha_{IIb}\beta_3$ (C). This suggests, again, that upon S-nitrosylation Mn^{2+}-activated $\alpha_{IIb}\beta_3$ reverts back toward a more native, resting conformation.

The Biotin-Switch Assay Reveals Nitrosylation of the Platelet Integrin $\alpha_{IIb}\beta_3$. In order to confirm the direct interaction between NO and $\alpha_{IIb}\beta_3$ identified in this study, and to ascertain if the platelet integrin is directly S-nitrosylated in vitro, we examined the interaction of NO and purified $\alpha_{IIb}\beta_3$ in the biotin-switch assay (*23*) as shown in Figure 6. An increase in the intensity of anti-biotin antibody binding is clearly seen in the NO-treated lane (lane 2), indicating that nitrosylation has occurred. The increase is most intense in the band seen at 90 kDa, which is the approximate mass of nonreduced β_3. There is also an increase in intensity of a higher band at approximately 180 kDa, which could indicate nitrosylation of a β_3 dimer. It is notable that there is no obvious band at 125 kDa corresponding to the α_{IIb} integrin subunit.

DISCUSSION

This study reveals the importance of the role of disulfide shuffling in the activation of the integrin $\alpha_{IIb}\beta_3$ and how S-nitrosylation regulates conformational changes in this receptor. We show that modification of $\alpha_{IIb}\beta_3$ by NO occurs through a direct interaction with its cysteine residues. S-Nitrosylation of the activated integrin alters the conformation of $\alpha_{IIb}\beta_3$ back toward a more nonactive state, as if this process is essentially switching the integrin "off". These data validate previous findings, where NO directly regulates the activation status of $\alpha_{IIb}\beta_3$ in the platelet and modulates its enzymatic thiol isomerase activity (*4*). Interestingly, S-nitrosylation can accelerate disulfide formation in the case of vicinal thiols (*29*), and so it is tempting here to speculate that S-nitrosylation of $\alpha_{IIb}\beta_3$ accelerates a disulfide reshuffle via the thiol isomerase activity of the activated integrin. The β_3 subunit contains nine vicinal motifs, in the form Cys-X-X-Cys (CXXC), and these motifs are thought to be the site of this activity in the subunit (*2*).

The extracellular portion of the β_3 subunit is of paramount importance in the conformational changes occurring in $\alpha_{IIb}\beta_3$ upon activation. This is particularly true of the EGF-like domains, a series of four cysteine-rich repeats which have been described as the "fulcrum" for the dramatic conformational changes that occur and form a cysteine-rich core in the more C-terminus end of the subunit (*30*). Although their exact identity remains enigmatic, the disulfides reduced upon activation are believed to reside in the EGF-like domain. All but two of the nine vicinal CXXC motifs in β_3 are found in these EGF-like domains and so are ideally located to play a role in activation or deactivation of the integrin. As NO regulates thiol isomerase activity of the integrin in an allosteric manner (*4*), it can be postulated that the thiol(s) which are S-nitrosylated may be at these remote N-terminus CXXC motifs away from the EGF domains. It is proposed that S-nitrosylation at one or both of these motifs can dictate the direction of the conformation of the integrin by allosterically regulating the thiol isomerase activity of the cysteine-rich core.

The presence or absences of free thiols are key markers of S-nitrosylation of $\alpha_{IIb}\beta_3$. In the case of native $\alpha_{IIb}\beta_3$ treated with NO, there appears to be loss of the SH groups, but this is difficult to ascertain as the signals are weak. However, when Mn^{2+}-activated $\alpha_{IIb}\beta_3$ is treated with NO, the disappearance of the SH groups is more striking and provides good evidence that NO is targeting free thiols in $\alpha_{IIb}\beta_3$ and binding to them. As expected, there are also major changes in C−S and S−S bonds in $\alpha_{IIb}\beta_3$. A population of strained disulfides is present in the native, resting $\alpha_{IIb}\beta_3$ that potentially represents a "spring". This disappears upon activation but partially reappears following a reversal of the activated state of $\alpha_{IIb}\beta_3$ by S-nitrosylation. This observation is consistent with the "switch blade" model of integrin activation, where in the presence of Mn^{2+} there is an outward swing of the hybrid domain of $\alpha_{IIb}\beta_3$ at the junction of the

I domain that results in a conformational change that allows ligand to bind (*31*).

S-Nitrosylation of cysteine residues with functional consequences has now been shown for many proteins, in a wide variety of cells and tissues, involved in many diverse cellular functions. Indeed, posttranslational modification of proteins by NO is now considered the prototypic redox-based signaling mechanism (*32*). The nucleophilic behavior of a thiol, and therefore its ability to trap NO, is dictated by its pK_a, which is strongly influenced by the cysteine neighbors. Correspondingly, S-nitrosylation occurs at specific, critical cysteines which are often located in an acid−base or hydrophobic structural motif (*33*, *34*). We examined the linear amino acid sequence of $\alpha_{IIb}\beta_3$, and while there was no motif present in the α_{IIb} subunit, we identified this motif four times in the extracellular portion of the β_3 subunit, at Cys-38, Cys-433, Cys-523, and Cys-581. Each of the motifs are in an acid/base amino acid configuration in that each of the potential cysteines that may be nitrosylated is flanked at position −1 by Arg, Asp, Glu, or Lys and at position +1 by either Asp or Glu. Interestingly, one motif is positioned in the N-terminus of the subunit while the remaining three motifs are grouped closely together in the cysteine-rich part of the EGF domains of the protein. However, the significance of this linear motif is as yet unclear, as the cysteine microenvironment and tertiary structure of the protein have recently been demonstrated to be more important than the linear sequence (*35*, *36*). The S-nitrosylation of $\alpha_{IIb}\beta_3$ was confirmed using the biotin-switch assay, which definitively showed S-nitrosylation of the β_3 subunit but not the α_{IIb} subunit, when treated with the NO donor, *S*-nitroso-*N*-acetylcysteine (SNOAC).

In addition to the observations from the Raman study and the finding that purified $\alpha_{IIb}\beta_3$ is subject to S-nitrosylation as demonstrated by the biotin-switch assay, flow cytometry analysis revealed that NO can specifically modulate the activation state of $\alpha_{IIb}\beta_3$ in situ in the platelet. Treatment of thrombin-activated platelets with NO and GSH causes a specific reversal of the activation state of $\alpha_{IIb}\beta_3$, without having an effect on general platelet secretion. This finding demonstrates that integrin activation can be modulated at the platelet surface, through a direct modification of the extracellular portion of $\alpha_{IIb}\beta_3$, independent of cGMP or other intracellular mediators.

This Raman analysis of $\alpha_{IIb}\beta_3$ reveals a direct interaction between NO and its cysteine residues. Raman spectroscopy is a rapid, real-time technique. Therefore, it has vast potential for use in novel assays to monitor changes in response to biochemical modulators of integrin activity. The findings of this study provide critical information regarding the regulation of the integrin $\alpha_{IIb}\beta_3$ by nitric oxide. We propose that Mn^{2+} activation of $\alpha_{IIb}\beta_3$ operates by releasing highly strained disulfides, possibly at vicinal cysteine sites, that reside within the native conformation of the integrin. NO can mediate disulfide re-formation of strained disulfides driven possibly by the greater nucleophilicity of the cysteines present in CXXC motifs. This interaction then regulates, in an allosteric manner, the conformation of the integrin. $\alpha_{IIb}\beta_3$ is a crucial component in the development of thrombotic disorders, but recent attempts to develop drugs specifically targeting this protein have proven unsuccessful. The structural findings of this study, combined with the discovery of the integrin's direct regulation by NO, will potentially aid the development of targeted antithrombotic therapies.

REFERENCES

1. Shattil, S. J. (1999) Signalling through platelet integrin alpha IIb beta 3: inside-out, outside-in, and sideways, *Thromb. Haemostasis 82*, 318−325.
2. O'Neill, S., Robinson, A., Deering, A., Ryan, M., Fitzgerald, D. J., and Moran, N. (2000) The platelet integrin alpha IIb beta 3 has an endogenous thiol isomerase activity, *J. Biol. Chem. 275*, 36984−36990.
3. Essex, D. W., and Li, M. (2003) Redox control of platelet aggregation, *Biochemistry 42*, 129−136.
4. Walsh, G. M., Sheehan, D., Kinsella, A., Moran, N., and O'Neill, S. (2004) Redox modulation of integrin [correction of integin] alpha IIb beta 3 involves a novel allosteric regulation of its thiol isomerase activity, *Biochemistry 43*, 473−480.
5. Yan, B., and Smith, J. W. (2000) A redox site involved in integrin activation, *J. Biol. Chem. 275*, 39964−39972.
6. Litvinov, R. I., Nagaswami, C., Vilaire, G., Shuman, H., Bennett, J. S., and Weisel, J. W. (2004) Functional and structural correlations of individual alphaIIbbeta3 molecules, *Blood 104*, 3979−3985.
7. Smith, J. W., Piotrowicz, R. S., and Mathis, D. (1994) A mechanism for divalent cation regulation of beta 3-integrins, *J. Biol. Chem. 269*, 960−967.
8. Yan, B., Hu, D. D., Knowles, S. K., and Smith, J. W. (2000) Probing chemical and conformational differences in the resting and active conformers of platelet integrin alpha(IIb)beta(3), *J. Biol. Chem. 275*, 7249−7260.
9. Xiao, T., Takagi, J., Coller, B. S., Wang, J. H., and Springer, T. A. (2004) Structural basis for allostery in integrins and binding to fibrinogen-mimetic therapeutics, *Nature 432*, 59−67.
10. Xiong, J. P., Stehle, T., Zhang, R., Joachimiak, A., Frech, M., Goodman, S. L., and Arnaout, M. A. (2002) Crystal structure of the extracellular segment of integrin alpha V beta 3 in complex with an Arg-Gly-Asp ligand, *Science 296*.
11. Xiong, J. P., Stehle, T., Diefenbach, B., Zhang, R., Dunker, R., Scott, D. L., Joachimiak, A., Goodman, S. L., and Arnaout, M. A. (2001) Crystal structure of the extracellular segment of integrin alpha V beta 3, *Science 294*, 339−345.
12. Chowdhury, M. H., Gant, V. A., Trache, A., Baldwin, A., Meininger, G. A., and Cote, G. L. (2006) Use of surface-enhanced Raman spectroscopy for the detection of human integrins, *J. Biomed. Opt. 11*, 024004.
13. Gaber, B. P., Sheridan, J. P., Bazer, F. W., and Roberts, R. M. (1979) Resonance Raman scattering from uteroferrin, the purple glycoprotein of the porcine uterus, *J. Biol. Chem. 254*, 83040−83042.
14. Keyes, T. E., Leane, D., Forster, R. J., Moran, N., and Kenny, D. (2005) New Insights into the molecular mechanisms of thrombosis from high resolution surface enhanced Raman microscopy, *Proc. Int. Soc. Opt. Eng., Opt. Sensing Spectrosc. 5826*, 221.
15. Kopecky, V., Jr., Ettrich, R., Hofbauerova, K., and Baumruk, V. (2003) Structure of human alpha1-acid glycoprotein and its high-affinity binding site, *Biochem. Biophys. Res. Commun. 300*, 41−46.
16. Tomimatsu, Y., Scherer, J. R., Yeh, Y., and Feeney, R. E. (1976) Raman spectra of a solid antifreeze glycoprotein and its liquid and frozen aqueous solutions, *J. Biol. Chem. 251*, 2290−2298.
17. Immoos, C. E., Sulc, F., Farmer, P. J., Czarnecki, K., Bocian, D. F., Levina, A., Aitken, J. B., Armstrong, R. S., and Lay, P. A. (2005) Bonding in HNO-myoglobin as characterized by X-ray absorption and resonance Raman spectroscopies, *J. Am. Chem. Soc. 127*, 814−815.
18. Li, D., Stuehr, D. J., Yeh, S. R., and Rousseau, D. L. (2004) Heme distortion modulated by ligand-protein interactions in inducible nitric-oxide synthase, *J. Biol. Chem. 279*, 26489−26499.
19. Rousseau, D. L., Li, D., Couture, M., and Yeh, S. R. (2005) Ligand-protein interactions in nitric oxide synthase, *J. Inorg. Biochem. 99*, 306−323.
20. Tomita, T., Ogura, T., Tsuyama, S., Imai, Y., and Kitagawa, T. (1997) Effects of GTP on bound nitric oxide of soluble guanylate cyclase probed by resonance Raman spectroscopy, *Biochemistry 36*, 10155−10160.

21. Pelton, J. T., and McLean, L. R. (2000) Spectroscopic methods for analysis of protein secondary structure, *Anal. Biochem. 277*, 167−176.
22. Yan, B., and Smith, J. W. (2001) Mechanism of integrin activation by disulfide bond reduction, *Biochemistry 40*, 8861−8867.
23. Jaffrey, S. R., and Synder, S. H. (2001) The biotin switch method for the detection of S-nitrosylated proteins, *Sci. STKE PL1*.
24. Jaffrey, S. R., Erdjument-Bromage, H., Ferris, C. D., Tempst, P., and Snyder, S. H. (2001) Protein S-nitrosylation: a physiological signal for neuronal nitric oxide, *Nat. Cell Biol. 3*, 193−197.
25. Jia, L., Young, X., and Guo, W. (1999) Physicochemistry, pharmacokinetics, and pharmacodynamics of S-nitrosocaptopril crystals, a new nitric oxide donor, *J. Pharm. Sci. 88*, 981−986.
26. Van Wart, H. E., Lewis, A., Scheraga, H. A., and Saeva, F. D. (1973) Disulfide bond dihedral angles from Raman spectroscopy, *Proc. Natl. Acad. Sci. U.S.A. 70*, 2619−2623.
27. Torreggiani, A., and Fini, G. (1998) The binding of biotin analogues by streptavidin: A Raman spectroscopic study, *Biospectroscopy 4*, 197−208.
28. Fleury, F., Ianoul, A., Kryukov, E., Sukhanova, A., Kudelina, I., Wynne-Jones, A., Bronstein, I. B., Maizieres, M., Berjot, M., Dodson, G. G., Wilkinson, A. J., Holden, J. A., Feofanov, A. V., Alix, A. J., Jardillier, J. C., and Nabiev, I. (1998) Raman and CD spectroscopy of recombinant 68-kDa DNA human topoisomerase I and its complex with suicide DNA-substrate, *Biochemistry 37*, 14630−14642.
29. Arnelle, D. R., and Stamler, J. S. (1995) NO^+, NO, and NO^- donation by S-nitrosothiols: implications for regulation of physiological functions by S-nitrosylation and acceleration of disulfide formation, *Arch. Biochem. Biophys. 318*, 279−285.
30. Beglova, N., Blacklow, S. C., Takagi, J., and Springer, T. A. (2002) Cysteine-rich module structure reveals a fulcrum for integrin rearrangement upon activation, *Nat. Struct. Biol. 9*, 282−287.
31. Takagi, J., Petre, B. M., Walz, T., and Springer, T. A. (2002) Global conformational rearrangements in integrin extracellular domains in outside-in and inside-out signaling, *Cell 110*, 599−611.
32. Stamler, J. S., Lamas, S., and Fang, F. C. (2001) Nitrosylation: the prototypic redox-based signaling mechanism, *Cell 106*, 675−683.
33. Gow, A. J., and Stamler, J. S. (1998) Reactions between nitric oxide and haemoglobin under physiological conditions, *Nature 391*, 169−173.
34. Stamler, J. S., Toone, E. J., Lipton, S. A., and Sucher, N. J. (1997) (S)NO signals: translocation, regulation, and a consensus motif, *Neuron 18*, 691−696.
35. Ascenzi, P., Colasanti, M., Persichini, T., Muolo, M., Polticelli, F., Venturini, G., Bordo, D., and Bolognesi, M. (2000) Reevaluation of amino acid sequence and structural consensus rules for cysteine-nitric oxide reactivity, *J. Biol. Chem. 381*, 623−627.
36. Hao, G., Derakhshan, B., Shi, L., Campagne, F., and Gross, S. S. (2006) SNOSID, a proteomic method for identification of cysteine S-nitrosylation sites in complex protein mixtures, *Proc. Natl. Acad. Sci. U.S.A. 103*, 1012−1017.

BI0620712